SLAC–PUB–4974
May 1989
(A)

MONITORING IN FUTURE e^+e^- COLLIDERS*

ROGER A. ERICKSON

Stanford Linear Accelerator Center

Stanford University, Stanford, California 94309 USA

1. INTRODUCTION

Study groups throughout the world have recently been examining possible parameter choices for a TeV-class linear collider.[1,2,3] In all cases, they have concluded that in order to achieve useful luminosity within plausible cost constraints, the opposing beams of electrons and positrons must be focused to extraordinarily small spots and steered into collision with an unprecedented degree of accuracy. Some means of monitoring these beam parameters will be essential in order to guide the focusing and steering. In this talk, examples will be presented which illustrate the nature of these new requirements, along with a discussion of the limitations of conventional techniques for monitoring such beams and some recent measurements from the SLAC Linear Collider[4] (SLC) that show how the next level of resolution in beam monitoring will be achieved.

2. THE REQUIREMENTS

The luminosity of a collider is given approximately by the expression

$$\mathcal{L} = \frac{1}{4\pi} \frac{f N^+ N^-}{\sigma_x \sigma_y} H_D \tag{1}$$

where N^+ and N^- are the numbers of positrons and electrons per bunch, f is the

Invited talk presented at the 3rd Joint US–CERN School on Particle Accelerators: Frontiers of Particle Beams, Observation, Diagnosis, and Correction, Capri, Italy, October 20–26, 1988.

⋆ Work supported by the Department of Energy, contract DE–AC03–76SF00515.

frequency of collisions, and σ_x and σ_y are the RMS radii of the bunches in the horizontal and vertical dimensions, respectively, at the interaction point (IP). H_D is a multiplicative factor that accounts for any mutual pinch effect that may enhance the luminosity as the beams pass and disrupt each other. Five sets of collider parameters are listed in Table 1. The values listed in the first column have been achieved at the SLC; all others are design studies. In all five machines, the numerator, fN^+N^-, is easy to measure continuously and nonintrusively by conventional techniques, such a toroid current transformers, E-field pickup electrodes, gap monitors, and the like. Monitoring σ_x and σ_y will require new and less direct methods because of the very small dimensions and high charge densities expected.

Table 1. Parameters of real and imagined linear colliders.

	SLC (9/88)	SLC Design[4]	TLC[1]	CLIC[2]	$B\overline{B}$ Factory[3]
E_{beam} (GeV)	46.	50.	500.	1000.	10.
$N^{\pm}$/pulse	$1. \times 10^{10}$	7.2×10^{10}	1.3×10^{10} ($\times$10 bunchlets)	0.5×10^{10}	$8. \times 10^{10}$
f (sec^{-1})	30.	180.	408.	1690.	12,000.
δp/p	0.3%	0.5%	0.14%	0.08%	0.1%
β_x^* (mm)	30.	5.	19.	7.0	4.0
β_y^* (mm)	30.	5.	0.085	0.282	4.0
σ_x^* (mm)	5.	1.6	0.3	0.06	0.6
σ_y^* (mm)	4.	1.6	0.0026	0.012	0.6
Aspect ratio	1.	1.	123.	5.	1.
$\mathcal{L}$ (cm^{-2} sec^{-1})	1.2×10^{27}	$6. \times 10^{30}$	8.2×10^{33}	1.1×10^{33}	$1. \times 10^{34}$

Equation 1 is an approximation for an ideal machine and neglects the fact that the spot size changes along the bunch length due to the geometric properties of the beam envelope near the focal point. Furthermore, it is assumed that the beams are Gaussian in their transverse distributions, that they are the same size and shape, that they are oriented the same way, and that they are steered exactly into collision. None of these assumptions is met without accurately monitoring and correcting the beam parameters. Each requires that the characteristics of both beams be observed while the machine is tuned, and that they be monitored while the machine is running to verify that all is working correctly.

The minimum achievable spot size depends on the momentum spread of the beam, the cumulative effects of magnetic field and alignment errors, and uncorrected high-order aberrations, among other considerations, and can be expressed approximately as:

$$\begin{aligned} \sigma^2 = \; & \epsilon\beta^* \\ & + \text{dispersion terms } [(\delta p/p)^2] \\ & + \text{skew terms } [x, y \text{ coupling}] \\ & + \text{higher-order chromatic terms} \\ & + \text{higher-order geometric terms} \quad . \end{aligned} \tag{2}$$

In this expression, ϵ is the emittance, β^* is the value of the beta function at the interaction point (IP), and δp is the rms momentum spread. A linear collider must be designed to deliver beams of the smallest possible emittance, focus them to the smallest practical β^*, and cancel the aberrations represented by each of the other terms in the expression above. Second-order chromatic effects, which become large whenever $\beta^*/f < \delta$p/p, are introduced mainly in the final stage of demagnification. Compared to the natural geometric beam size $\sqrt{\epsilon\beta}$, the higher-order effects are significant only at the IP, where they dominate the spot size unless they are compensated using sextupoles and other special optical elements. At the SLC, these aberrations typically add about 10 μm to the final spot size after the orbits have been steered and first-order optical corrections have been performed using diagnostic devices upstream of the final quadrupoles.[5] Only after precise tuning, guided by observations of the beams at the IP, have spot sizes in the 2 μm range been achieved.[6]

In a realistic design, the various aberrations are mixed to the extent that separate measurements and orthogonal corrections for each are impractical. Thus, an important part of any new collider design must be a tuning procedure that converges quickly on a configuration in which all significant aberrations are reduced to an acceptable level. The success of the next linear collider may well depend on whether suitable monitoring techniques can be developed to guide this procedure.

3. CONVENTIONAL MONITORING DEVICES

3.1 Bhabha Scattering

The e^+e^- elastic ("Bhabha") scattering rate has been a useful figure of merit for conventional storage rings. The Bhabha rate can be calculated from fundamental principles with high accuracy, and thus gives an absolute measure of luminosity. The scattering rate into an angular region bounded by θ_{min} and θ_{max} is $R = \mathcal{L}\Delta\sigma$, where

$$\Delta\sigma = \frac{4\pi\alpha^2}{E^2}\left(\frac{1}{\theta_{min}^2} - \frac{1}{\theta_{max}^2}\right) \tag{3}$$

is the Bhabha cross section, E is the energy of each beam, and α is the fine structure constant. Note that the Bhabha scattering rate falls as $1/E^2$. Table 2 lists the Bhabha rates that would be expected in the various colliders equipped with a two-level detector system similar to the Mark II "miniSAM" and "SAM" small-angle shower monitors at SLAC.

Table 2. Bhabha scattering rate (events/sec) into the angular ranges $15 < \theta < 25$ and $50 < \theta < 150$ mrad for each of the machines in Table 1.

	SLC (9/88)	SLC Design	TLC	CLIC	$B\overline{B}$ Factory
Range (mrad)					
$15 < \theta < 25$	4.2×10^{-4}	1.8	24.	0.81	7.4×10^4
$50 < \theta < 150$	0.5×10^{-4}	0.2	3.	0.10	0.9×10^4

The Bhabha rate is high enough in the $B\overline{B}$ Factory that it would be useful as a real-time monitor. Even though it is only a single scalar quantity, it is a measurable quantity that is directly proportional to the quantity of interest: the luminosity. In the TeV-class machines, however, Bhabha counting may be useful for confirming either that a collider is working, or for normalizing data offline, but the rate is too slow to be of much value in guiding the tuning procedures. In any case, the design of a suitable Bhabha detector to cover either of the angular ranges listed may be problematical in a machine with quadrupoles located very near the IP ($l^* = 40$ cm in the TLC design). For the TeV machines, other monitoring techniques will be essential.

3.2 Fluorescent Screens

Profile monitors, based on a fluorescent screen inserted in the path of the beam and viewed by a TV camera, have proven to be immensely valuable for many accelerator applications, including many places in the SLC.[7,8] Such a monitor was even used at the SLC interaction point at an early stage in the commissioning. They have been used for diagnosing hardware problems, verifying the proper operation of magnets, measuring emittance, and tuning out cross-plane coupling. The images are easy to interpret, and they are unsurpassed for diagnosing skewed or distorted beam spot shapes. Furthermore, apparatus for digitizing and processing video images is commercially available and easily integrated into the accelerator control system to measure emittance and other beam parameters. An example of a video image of a beam profile near the end of the SLAC linac is shown in Fig. 1. The digitized projection of this image is shown in Fig. 2. Resolutions of 50 μm are routinely achieved, and the prospect of reaching 10 μm resolution with this technique seems likely. Beyond this point, the diffraction limits of camera lenses and the graininess of fluorescent screens become important.

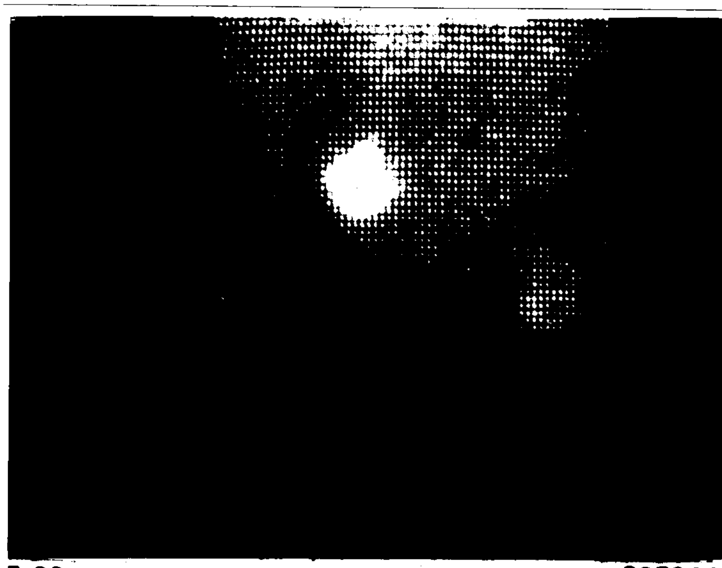

7-88 6059A3

Fig. 1: Electron beam profile at 47 GeV on a profile monitor at the end of the SLAC linac. The central white spot is the beam image, the grid of white dots the digitization points, and the dark dots the fiducial holes, spaced 3 mm horizontally and 1 mm vertically.[8]

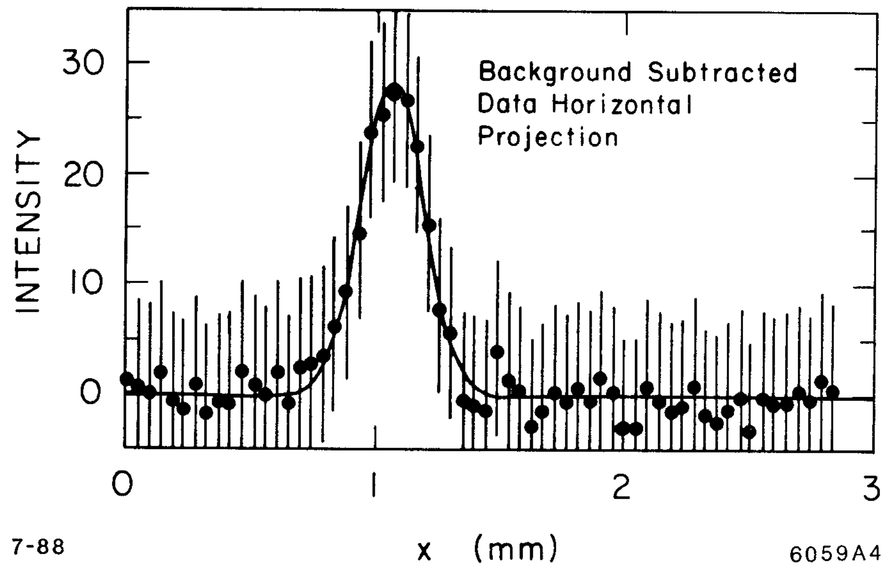

Fig. 2: Projected profile of the digitized beam image in Fig. 1.

At least a dozen different screen materials have been tested at SLAC.[9] Some, such as variations of the traditional zinc sulfide screen, are easily damaged by ionizing radiation and quickly become unusable. Others, including various commercially made materials on plastic substrates, are bright and have good resolution, but cannot be used in high-vacuum systems. Two materials have been in wide use at SLAC; one is a chromate-activated alumina, which is robust and radiation resistant but somewhat grainy; the other is based on activated gadolinium oxide, Gd2O2S:Tb. Both are usually deposited on aluminum substrates, although ceramic substrates have been used successfully both at SLAC and at CERN.[10] At the SLC, the gadolinium oxide screens have given the best results in the applications with the most demanding resolution requirements.

In tests with a high-energy electron beam, all materials tested at SLAC show damage when exposed to 2.5×10^{10} electrons/μm^2, some severely so. In a typical SLC application, the beam current is reduced to 2×10^9 electrons/pulse and the repetition rate is reduced to 10 pulses/sec. A typical linac-size beam then deposits about $1.5 \times 10^4 e^-/\mu\text{m}^2$/pulse, and thus can be used for more than 10^5 seconds before the screen needs replacement. When used for brief and infrequent measurements, such a screen lasts for a long time in many SLC applications (but not at the IP!).

Consider the application of fluorescent screens at the focus of any of the future machines listed in Table 1. The particle density at the focal point of the TLC, for example, is about 5×10^{12} particles/μm^2/pulse. A single pulse from any of the machines listed would destroy the active surface of any conventional screen. It would be interesting to consider a "screen-strip" that rolls by continuously, like the film in a movie projector. The beam would punch a row of holes in the strip, which could conceivably be examined with a microscope.

Quite apart from the survivability problem, a fundamental resolution limit is imposed by the wave nature of light. The rms spot size of the $B\overline{B}$ Factory—the largest among the future machines listed—is equal to only one wavelength of visible light. The TLC and CLIC beams have horizontal widths corresponding to a single wavelength of ultraviolet light, and vertical sizes of only 26 Å and 126 Å, respectively. No monitor using optical devices to "see" the beam spot will be of any use for these applications.

3.3 Wire Scanners

Another approach to monitoring small spot sizes is based on the interaction of a beam with a thin wire stretched across its path. The beam size can be determined by detecting either the secondary emission signal directly from the wire or the bremsstrahlung radiation emitted as the beam is scanned across the wire. A device using carbon fibers as small as 4 μm in diameter has been used successfully at the IP of the SLC and continues to be an essential tool for tuning the final focus.[11]

The spot size observed with this technique is given by

$$\sigma^2_{measured} = \sigma^2_{beam} + r^2_{wire}/n \tag{4}$$

where n has a value of approximately 3 to 4, depending on the detection method and the charge of the beam particles. The secondary emission method, which is based on ejecting electrons from the surface of the wire, is particularly sensitive to the charge of the beam. The signal induced by a positron beam is about five times as strong as that from an electron beam, and the apparent beam width is significantly greater. Bremsstrahlung radiation, on the other hand, is produced by high-energy interactions throughout the volume of the wire, and thus is free of most of these systematic difficulties. Bremsstrahlung radiation is emitted in the direction of the incident beam, with essentially the same angular spread. In the SLC design, this radiation is intercepted by special detectors located along a line-of-sight from the IP, just upstream of the last large dipole bending magnet on each side as shown in Fig. 3. By deconvoluting the wire size from the observed spot size, the actual spot size can be determined with an accuracy of less than 1 μm, depending on how well the wire diameter is known, how precisely the beam can be scanned across the wire, and how stable the incoming beam is during the scanning process. Figure 4 shows an example of a positron beam vertical profile measured with a 4 μm wire by detection of the bremsstrahlung radiation.

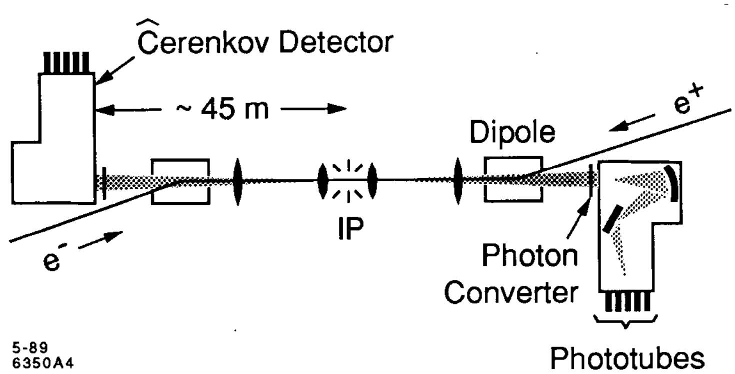

Fig. 3: Gas Čerenkov detectors are used at the SLC to monitor bremsstrahlung radiation from either beam colliding with a carbon fiber at the IP, or beamstrahlung radiation from the beams colliding with each other (schematic representation not drawn to scale).

An important limitation on the usefulness of the wire-scanning technique is the survivability of the fiber when struck by the charged particle beam. There are at least two beam-induced failure modes: breaking due to the thermal expansion shock induced by a virtually instantaneous temperature rise of more than 1000° C , and melting (or evaporation) when the temperature exceeds the melting point. Carbon is the material of choice because of its low atomic number (and thus low energy deposition by ionizing particles) and its high melting point (about 3550° C). Carbon fibers are also very strong and are commercially available in the small diameters of interest here. A single beam

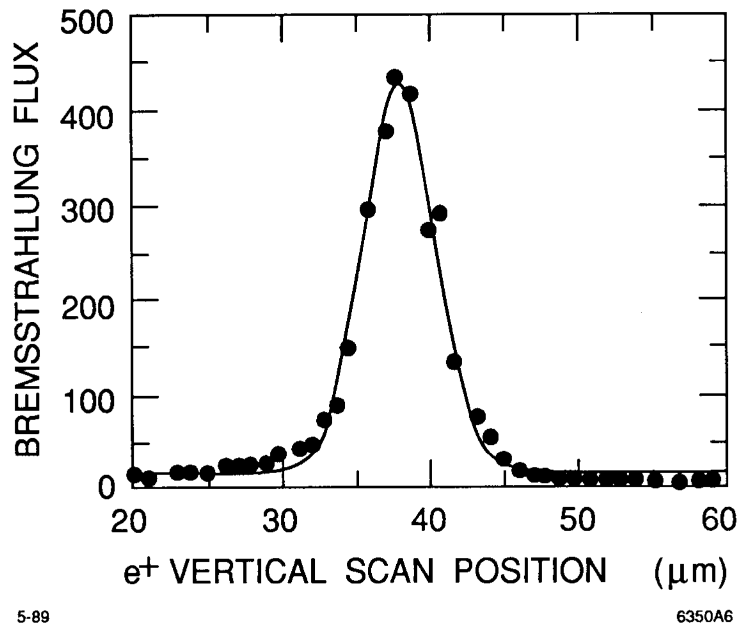

Fig. 4: Vertical profile of the SLC positron beam, measured at the interaction point with a 4 μm carbon fiber. The solid line is a Gaussian fit to the data, showing an apparent spot size of σ_y = 2.4 μm. Deconvoluting the wire diameter yields an actual beam size of σ_y = 2.1 μm.

pulse of about 1.7×10^{10} particles incident on a carbon fiber with a spot size σ of 3 μm will raise the temperature to the melting point.

Fibers of various sizes up to about 35 μm in diameter have been used successfully for many hours in the SLC with no evidence of damage at beam intensities up to several times 10^9 particles per pulse and a repetition rate of 10 pulses/sec. However, 4 and 7 μm fibers have been broken in recent weeks when the beam intensity exceeded 10^{10} particles/pulse with a spot size on the order of 5 μm. An interlock system has been added to the SLC control system which automatically limits the repetition rate to 10 pulses/second and the intensity to less than 1×10^{10} particles/pulse whenever one of the carbon fibers is moved to a position where it can be hit by the beam. A reduced-intensity and reduced-rate tuning mode may prove to be an essential feature for the next linear collider as well.

4. MONITORING WITH BEAM-BEAM EFFECTS

4.1 Beam-Beam Deflections

The electromagnetic force acting between two intense colliding beams of oppositely charged particles will cause them to be deflected in passing by an angle that depends on the offset between the bunches and the distribution of charge within the bunches. This deflection, measurable with nonintercepting devices, is a powerful tool for guiding the tuning of microscopic beams and for steering them into collision.[12,13]

The deflection of a single "probe" particle of charge e, passing at an offset Δ from the centroid of an oppositely charged "target" bunch having a Gaussian distribution, is given by:

$$\theta(\Delta) \;=\; \frac{-2\, r_e\, N_T}{\gamma}\; \frac{1-\exp\left[\,-\Delta^2/2\sigma^2\right]}{\Delta} \quad , \tag{5}$$

where r_e is the classical radius of the electron, N_T the number of particles in the target bunch, σ is the RMS transverse size of the Gaussian distribution, and $\gamma = E/mc^2$.

When two beams pass with offsets large compared to their transverse sizes, they see each other as point charges; Eq. (5) is a good approximation for their mutual deflection. When colliding with a small offset, the sizes and shapes of both beams must be taken into account. This can be done by a convolution of the generalized single-particle deflection with the distribution of the probe beam. For the case of unequal but erect elliptical Gaussian distributions, the deflections in the x and y planes are given by[14]:

$$\langle\theta_{x,y}\rangle \;=\; \frac{-2\, r_e\, N_T\, \Delta_{x,y}}{\gamma} \int_0^\infty dt\; \frac{\exp\left\{-\dfrac{\Delta_x^2}{(t+2\Sigma_x^2)} - \dfrac{\Delta_y^2}{(t+2\Sigma_y^2)}\right\}}{(t+2\Sigma_{x,y}^2)\,(t+2\Sigma_x^2)^{1/2}\,(t+2\Sigma_y^2)^{1/2}} \quad , \tag{6}$$

where Δ_x and Δ_y are the distances between beam centers in the x and y dimensions, and $\Sigma_x^2 = \sigma_{P,x}^2 + \sigma_{T,x}^2$ and $\Sigma_y^2 = \sigma_{P,y}^2 + \sigma_{T,y}^2$ are the quadratic sums of the probe and target beam sizes. Note that this expression is symmetric with respect to the two beams. If the number of particles in two opposing bunches are equal, the deflections will be equal, as they must be to conserve the total momentum. The integration can be performed analytically for the special case of $\Sigma_x = \Sigma_y = \Sigma$, which includes round beams of unequal size. With $\Delta = \sqrt{\Delta_x^2 + \Delta_y^2}$, the result is:

$$\langle \theta_{x,y} \rangle \;=\; \frac{-2\, r_e\, N_T\, \Delta_{x,y}}{\gamma\, \Delta} \left(\frac{1 - \exp\left\{ -\dfrac{\Delta^2}{2\Sigma^2} \right\}}{\Delta} \right) \quad . \tag{7}$$

As expected, there is no deflection when the beams are far apart or when they are exactly centered. The maximum deflection for round beams occurs where the impact parameter is approximately 1.6 σ.

At the SLC, these deflections are measured using four strip-line beam-position-monitors (BPMs), two on either side of the IP, as shown in Fig. 5. The four electrodes in each BPM are carefully impedance-matched and read out at both ends,[15] exploiting their directional coupler properties to allow independent measurements of both the incoming and outgoing beams a few nanoseconds apart. The pulse-to-pulse resolution of these BPMs has been measured to be better than 10 μm for beam intensities of 5×10^9 particles/pulse, and improves with increased intensity.

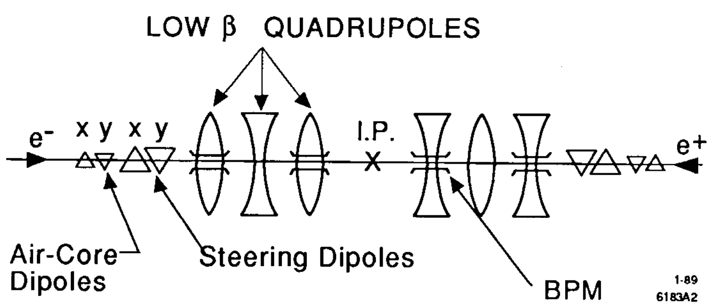

Fig. 5: Schematic of SLC beamline components relevant to the beam-beam deflection measurement.

Measuring the positions in two BPMs on each side defines the incoming and outgoing beam trajectories at the IP. The information from all four BPMs is used in four separate

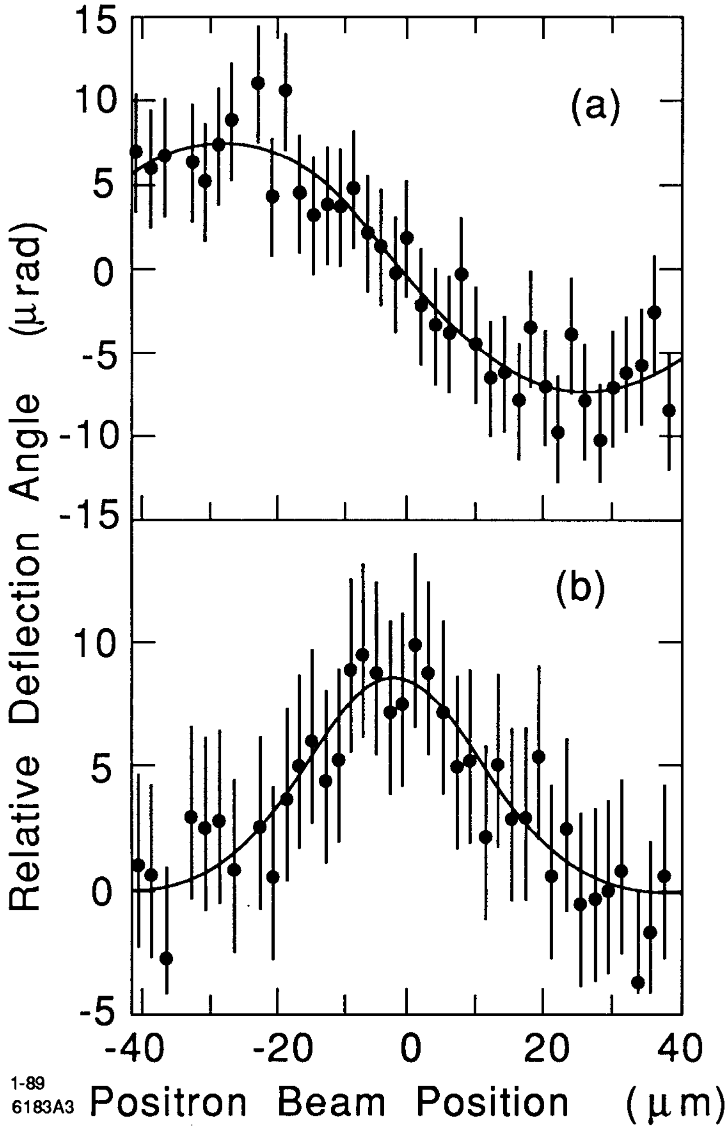

Fig. 6: A beam-beam deflection scan of the e^+ beam relative to its initial position showing (a) the in-plane deflection, and (b) the out-of-plane deflection. The e^- beam intensity was about 7×10^9 e^-/pulse, and both beams were approximately round with $\sigma = 7$ μm. The beams were approximately 10 μm apart in the out-of-plane direction during this scan.

linear fits to yield the beam position, the incoming angle, and the deflection angle (all evaluated at the IP) in each plane for both beams on a single beam pulse. While the positions and angles of the beams at the IP are observed to be stable on a pulse-by-pulse basis to a fraction of the measured beam size and angular divergence (typically

200–300 μrad), random fluctuations in the outgoing beam angle can still be several times larger than the expected maximum deflection. Fitting directly for the difference between the outgoing and incoming angles of a given beam effectively decouples any angular motion of the incoming beam from the deflection angle measurement.

In practice, the deflection angles for both beams are measured as a function of the impact parameter as one beam is swept across the other in either the horizontal or the vertical direction.[13] These beam scans are accomplished at the SLC using small air-core dipole magnets (Fig. 5), which can increment the beam position with a resolution of about 0.05 μm. Since the beams deflect each other very little when they are far apart, they must first be brought to within a few beam radii of each other. This has been done at the SLC by steering the beams, one at a time, onto the the carbon fiber wire-scanner device described above. After the beams are approximately centered in this way, the wire-scanner is retracted. To precisely center the beams, one beam is then scanned past the other, typically over a range of ± 40 μm in 2 μm steps. The BPM signals are processed on each pulse and correlated with the scan step position. The results of a typical beam scan are shown in Fig. 6. The deflection angles parallel and perpendicular to the scan direction are plotted in Figs. 6(a) and 6(b), respectively, as a function of the scanned beam's distance from its original position. For beams that are approximately round, the data are expected to be described by Eq. (7). For real-time beam centering, this expression is fit to the in-plane deflection measurements, assuming the beams were aligned in the scanning plane, while a Gaussian is fit to the out-of-plane deflection measurements. Curves showing these fits are superimposed on the data in Fig. 6.

Figure 7 shows deflection data obtained by scanning the e^+ beam in the y direction after centering the beams in x. The beam sizes were measured prior to this scan using the carbon filaments and found to be $\sigma_x = 7.2$ μm, $\sigma_y = 3.9$ μm for the electron beam and $\sigma_x = 4.9$ μm, $\sigma_y = 3.9$ μm for the positron beam. The curve overlaying the data is the result of a numerical calculation using the measured beam sizes as input. The overall normalization of the curve, which corresponds to the beam currents, was adjusted to fit the deflection data. The currents determined in this way are consistent with currents

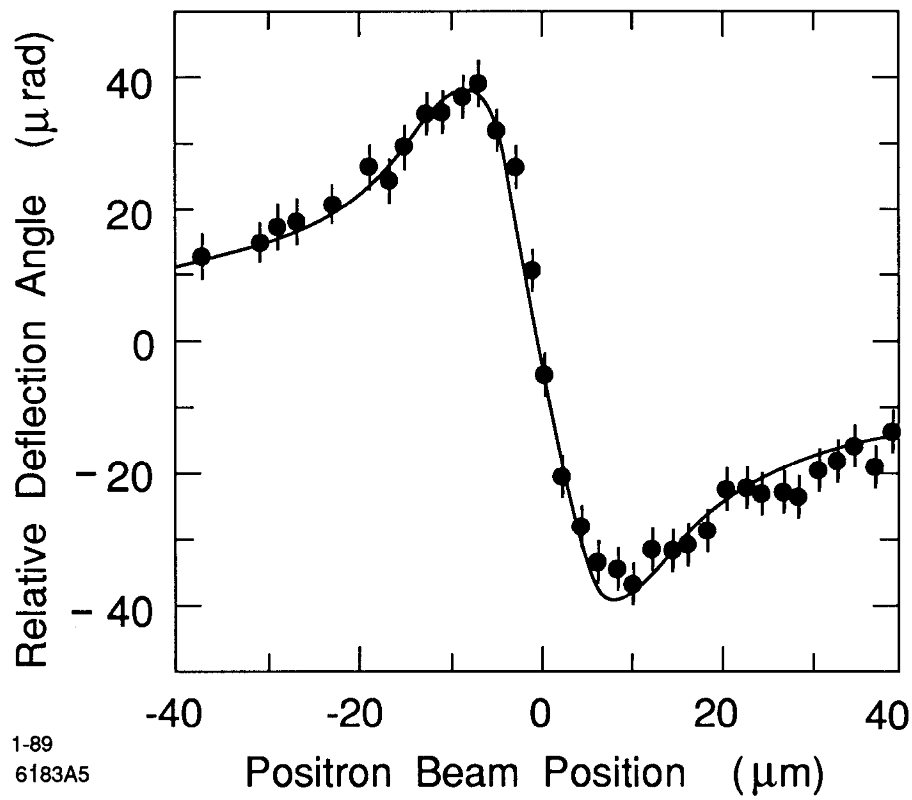

Fig. 7: An e^+ *beam deflection scan in y after alignment in x. The curve overlaying the data is a theoretical calculation using as input the beam sizes as measured by the wire filaments.*[13]

measured with other more conventional techniques.

Beam-beam deflections provide the standard method of steering the SLC beams into collision. Steering the scanned beam to the position corresponding to the zero-crossing of the deflection curve aligns the beams to a small fraction of the beam size. At the SLC collision point, the beam spots are approximately round, so meaningful fits to the deflection data using the form of Eq. (7) can be made. These immediately yield estimates of the beam sizes and intensities.

The slope of the deflection curve at the zero-crossing point is given by

$$S^P_{x,y} = \frac{2\,N_T\,r_e}{\gamma}\,\left[\Sigma_{x,y}\,(\Sigma_x + \Sigma_y)\right]^{-1} \quad . \tag{8}$$

This is a measurable parameter that is particularly useful for optimizing the luminosity, as demonstrated in Fig. 8, which shows the dependence of the slope on the x width of the e^- beam for several different e^+ beam radii. The electron beam size in y is assumed fixed near its optimal value.

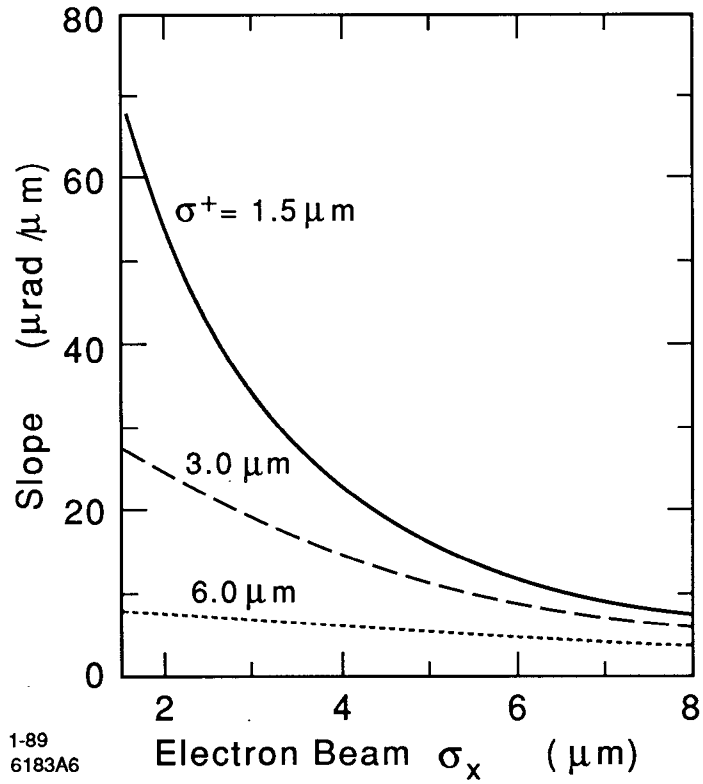

Fig. 8: The expected slope of the in-plane deflection curve at the zero-crossing point as a function of the e^- beam σ_x^- with a fixed σ_y^- of 1.5 μm. The solid curve corresponds to a round e^+ beam with $\sigma^+ = 1.5$ μm, the dashed to $\sigma^+ = 3.0$ μm and the dotted to $\sigma^+ = 6.0$ μm. The target beam intensity for these calculations was 1×10^{10}.

The relationship between the slopes of the deflection curves and the luminosity is[16]:

$$\mathcal{L} = \frac{N f \gamma}{4\pi r_e} (S_x + S_y) \quad , \tag{9}$$

where S_x and S_y are the slopes of the deflection curves measured with separate x and y scans after the beams have been centered. An independent measurement of the number of particles, N, in the deflected beam is also required to determine the luminosity. The advantage of using the slopes is that they can be accurately measured even when the beams are not round. Optimal luminosity can be achieved by adjusting the focus of the beams to obtain the maximum slopes. Once this has been established, it can be monitored by checking the slopes periodically with short scans across the zero-crossing point.

Figure 9 demonstrates how beam-beam deflections are used at the SLC for guiding an automatic focusing procedure. In this example, the waist of the positron beam was moved longitudinally by a programmed sequence of quadrupole strength adjustments, with the vertical size determined at each step by a deflection scan. An online fit to these measurements revealed the adjustment needed to focus the beam for optimum luminosity. Similar scans are routinely done for both beams to minimize both the vertical and horizontal spot sizes using the last set of quadrupoles before the IP, and to minimize the x, y coupling with a set of skew quadrupoles.

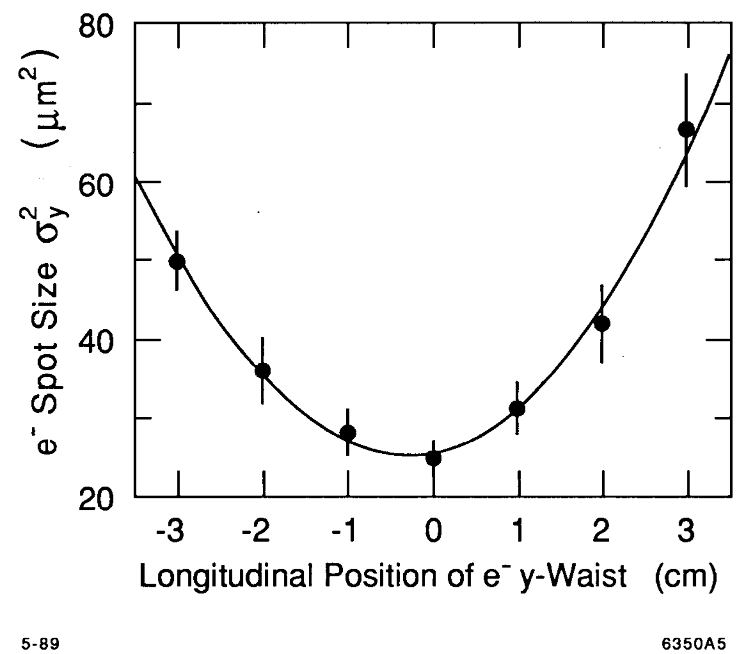

Fig. 9: Electron beam vertical spot size σ_y^2 as a function of the longitudinal position of the focus. Each datum was obtained with a beam-beam deflection scan, and the curve is a parabolic fit to these points. In this run, the minimum (σ_y = 5 μm) was seen to be close to the nominal interaction point.

The preceding discussion is applicable to opposing beams that are elliptical and erect (the axes of the opposing ellipses are parallel with the same x, y coordinate axes), but not necessarily the same size, shape, or density. The case of flat beams with arbitrary orientation is mathematically more complex, and is best studied by computer simulation. The interpretation of the deflections expected with flat beams of extreme aspect ratio (see Table 1), but imperfect azimuthal orientation, may prove to be challenging. This deserves further study.

4.2 Beamstrahlung Radiation

Beamstrahlung is the name given to the radiation emitted by a bunch of particles as it passes through the electromagnetic field of an opposing bunch. The radiation emitted by each particle in the bunch depends on the net force it feels in this passage.[17] Computer simulations suggest that this phenomenon could yield detailed information about the relative sizes and shapes of two opposing beams, if the beamstrahlung amplitude can be measured as the beams are scanned across each other along various axes.[18] The interpretation of such measurements is not likely to be obvious, however. For example, the conditions that lead to maximum beamstrahlung production do not necessarily lead to maximum luminosity. The maximum radiation is emitted by particles offset about 1.6 σ from the center, where the maximum beam-beam deflection occurs. In contrast, the maximum contribution to the luminosity comes from particles at the center of the bunch, where they are most likely to collide with particles of the opposing bunch.

For beams that are round and centered on each other, focusing them to increase the luminosity will also increase the beamstrahlung. On the other hand, if the beams are not round or if they are not centered, the maximum beamstrahlung will occur under conditions that may be far from the optimum luminosity conditions; indeed, as identical round beams are steered through each other, the beamstrahlung flux will dip as the beams become centered.

When two round Gaussian bunches collide head on, the radiated energy is given approximately by the classical synchrotron radiation formulation:

$$W \approx 0.2 \frac{r_e^3 N_P N_T^2 \gamma mc^2}{\sigma_z \sigma_r^2} \quad , \tag{10}$$

where σ_z and σ_r are the longitudinal and radial sizes of the bunches, respectively, and N_P and N_T are the numbers of particles in the probe and target bunches. For equal-size opposing beams, the number of photons emitted is proportional to $1/\sigma_r$, and the critical energy of the radiation spectrum is also proportional to $1/\sigma_r$. The radiation is peaked strongly forward in the direction of the beam motion.

Beamstrahlung is a macroscopic manifestation of beam-beam interactions that can be detected and quantified for each collision. In the SLC design, this radiation is intercepted by special detectors[19] located along a line-of-sight from the IP, just upstream of the last large dipole bending magnet on each side as shown in Fig. 3. The expected performance of the SLC beamstrahlung system is shown in Fig. 10.

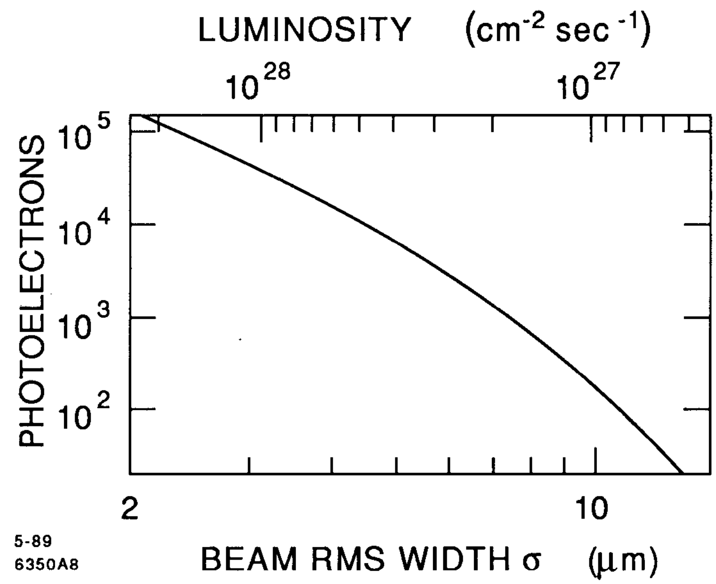

Fig. 10: Beamstrahlung flux expected in the SLC Čerenkov detectors as a function of spot size σfor equal round beams of 10^{10} particles per pulse. The units of the vertical scale are photoelectrons, as detected in the photomultiplier cluster. A luminosity scale is also shown, based on an assumed repetition rate of 120 Hz.[19]

These detectors, which are also used for detecting the bremsstrahlung radiation when the carbon fiber monitor is used as described above, contain a thin metal radiator which converts some of the energetic photons to e^+e^- pairs, which in turn radiate Čerenkov light in a volume of ethylene gas. The Čerenkov light is transmitted and focused by a set of mirrors onto an array of photomultiplier tubes. The challenge in designing such a detector is to make it sensitive to the beamstrahlung photons above a background of lower energy but far more numerous synchrotron radiation photons generated by the beams as they pass through the final focus magnets. The spectra of these photons are shown in Fig. 11. The Čerenkov threshold is determined by the gas pressure, which in the SLC detectors has been set to 0.3 atm, corresponding to a threshold of about 25 MeV, to give a detectable beamstrahlung signal while staying above the intense synchrotron radiation from the bend magnet ($E_{critical}$ = 2.2 MeV).

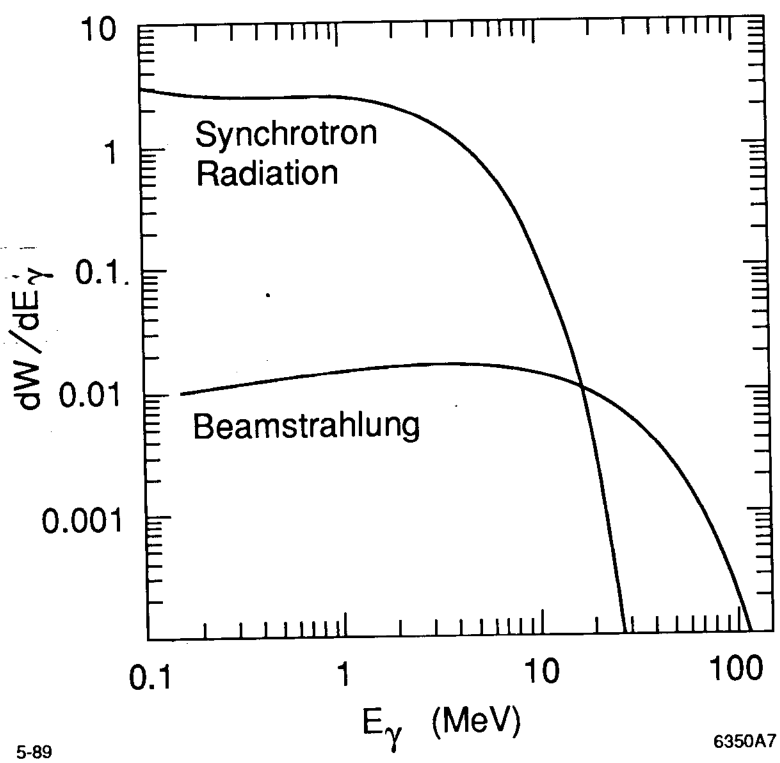

Fig. 11: Relative energy spectra of synchrotron radiation and beamstahlung expected at the SLC Čerenkov detectors. For this calculation, the assumed beam parameters were N = 10^{10}, σ_r = 4 μm, and σ_z = 1 mm.[19]

Figure 12 shows data from a beam-beam deflection scan and the corresponding signals from each of the two beamstrahlung detectors. The beam intensities were 1.4×10^{10} e^- per pulse and 1.0×10^{10} e^+ per pulse, and the spot size σ_r was approximately 5 microns

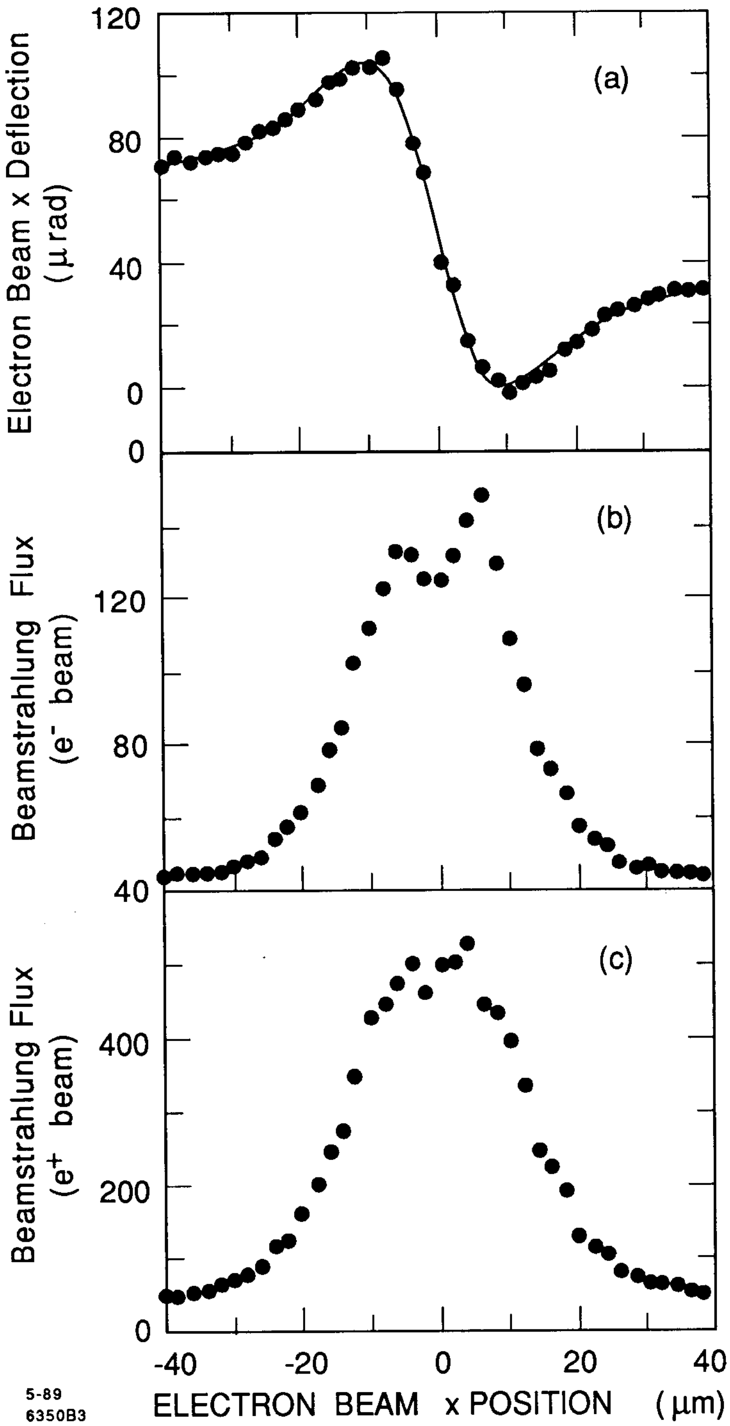

Fig. 12: Deflection curve (a) observed at the SLC as the elctron beam ($N = 1.4 \times 10^{10}$; $\sigma \approx 5\ \mu m$) was scanned horizontally across the positron beam ($N = 1.1 \times 10^{10}$; $\sigma \approx 5\ \mu m$) in 2 μm steps. The curve is a real-time fit, as described in the text. The beamstrahlung signals from the e^- beam and e^+ beam, as observed during the scan, are shown in parts (b) and (c). The vertical scales are ADC counts.

for both beams. Both beamstrahlung signals dipped as the beams passed through the optimum alignment point.

The small spot and high-luminosity parameters of the TeV-class collider studies lead to beamstrahlung fluxes that carry off a substantial fraction of the total beam energy. These machines enter the quantum beamstrahlung regime, where the classical synchrotron radiation formulation is no longer adequate. In the limit of very high-density bunches, the energy radiated is proportional to $\sigma_r^{-2/3}$. While the radiation intensity is quantitatively different in this high-disruption regime, the applicability to collision monitoring remains essentially the same.

5. CONCLUSIONS.

Establishing and maintaining the submicron spot sizes envisioned for future high-energy e^+e^- colliders will necessarily require sophisticated monitoring techniques. Profile monitor screens, wire scanners, and other conventional techniques that intercept the beam with solid materials have proven to be immeasurably valuable in a great variety of accelerator applications when the particle density is not too high and the spot sizes are not too small. At future e^+e^- colliders, however, these devices will not be able to withstand the destructive energy density of such beams, nor are they likely to achieve the resolution that will be required. On the other hand, such devices need only be adequate to guide beam tuning to the point where beam-beam effects become strong enough to give measurable signals in strip-line beam position monitors, radiation detectors, or other nonintercepting devices. Recent experience at the SLAC Linear Collider has demonstrated that this gap has been bridged. Beam sizes of several microns, and intensities of a few times 10^9 particles per pulse, recently shown to be within the capability limits of carbon-fiber scanners, also produce mutual beam-beam deflections and beamstrahlung radiation detectable at a level adequate to guide further tuning. As the beam spots get smaller and current intensities get higher, these signals become stronger and clearer, and intercepting devices become unnecessary. Calculations suggest that a great deal of information about the size, shape, and charge distribution of microscopic beams can be deduced from measurements of deflection angles and the properties of the emitted beamstrahlung radiation as the beams are scanned across each other and varied in size and current. Whether these techniques will be adequate for tuning future colliders with flat beams of miniscule thickness and large aspect ratios, while retaining the flatness, straightness, and orientation of such beams, remains to be demonstrated.

6. ACKNOWLEDGMENTS.

It is a pleasure to acknowledge H. DeStaebler, C. Field, E. Gero, W. A. Koska, K. Oide, J. M. Patterson, M. C. Ross, R. Ruth, J. T. Seeman, and S. R. Wagner, who all provided material and suggestions for this talk; and the present and former members of the SLC Final Focus Group, who developed and demonstrated much of the technology described here.

REFERENCES

1. R. B. Palmer *et al.,* SLAC TLC Study Group (May 1988), unpublished.
2. W. Schnell, CERN/LEP-RF/88-30 (June 1988).
3. U. Amaldi and G. Coignet, *Nucl. Inst. Methods* **A260** (1987).
4. SLC Design Handbook (December 1984).
5. R. Erickson, "Final Focus Systems for Linear Colliders," *AIP Conference Proceedings,* No. 184 (1989), R. Lerner, ed.
6. P. Bambade *et al.,* "Operational Experience with Optical Matching in the SLC Final Focus System," SLAC–PUB–4776 (1989).
7. M. C. Ross *et al.,* "High Resolution Beam Profile Monitors in the SLC," SLAC–PUB–3640 (1985).
8. J. T. Seeman and C. Adolphsen, SLAC–PUB–4642 (May 1988), contributed talk at the 1988 European Particle Accelerator Conference, Rome, Italy, June 7–11, 1988.
9. J. T. Seeman, V. Luth, M. Ross, and J. Sheppard, "Beam Tests of Phosphorescent Screens," SLAC CN–290 (March 1985), unpublished.
10. C. D. Johnson, SLAC CN–366 (July 1988), unpublished.
11. R. C. Field, "Problems of Measuring Micron-Size Beams," *Proceedings of the IEEE Particle Accelerator Conference,* Chicago, Illinois, March 20–23, 1989.
12. P. Bambade and R. Erickson, SLAC–PUB–3979 (May 1986), and *Proceedings of the 1986 Linear Accelerator Conference,* SLAC–Report–303 (September 1986).
13. P. Bambade, R. Erickson, W. A. Koska, W. Kozanecki, N. Phinney, and S. R. Wagner, SLAC–PUB–4767 (January 1989), submitted to *Phys. Rev. Letters.*
14. K. Hirata, *Nucl. Instr. Methods* **A269** 7 (1988).
15. J.-C. Denard, G. B. Bowden, G. J. Oxoby, J.-L. Pellegrin, M. C. Ross, "Monitoring the Beam Position in the SLC Interaction Region," SLAC–PUB–4267 (March 1987), presented at the Particle Accelerator Conference, Washington, D.C., March 16–19, 1987.
16. Thanks to H. DeStaebler and W. A. Koska for pointing out this useful relationship.
17. For a comprehensive introduction to beamstrahlung, see P. Chen, *Proceedings of the Joint US–CERN School on Particle Accelerators, Frontiers of Particle Beams;* published in Springer-Verlag *Lecture Notes in Physics,* No. 296 (1988).
18. E. Gero, G. Bonvicini, W. Koska, C. Field, "Beamstrahlung as an Optics Tuning Tool at the SLC IP," SLAC–PUB–4930 (March 1989), presented at the IEEE Particle Accelerator Conference, Chicago, Illinois, March 20–23, 1989.

19. G. Bonvicini, R. Frey, E. Gero, W. Koska, C. Field, A. Minten, "A Monitor for Gamma Radiation at Zero Degrees from the SLC Collision Point," SLAC–PUB–4735 (October 1988), to be published.